Oncogene (2011) 1–14

www.nature.com/onc

ORIGINAL ARTICLE

Introduction of SV40ER and hTERT into mammospheres generates breast cancer cells with stem cell properties

AN Paranjape[1,2], T Mandal[1], G Mukherjee[2], MV Kumar[2], K Sengupta[3] and A Rangarajan[1]

[1]*Department of Molecular Reproduction, Development and Genetics, Indian Institute of Science, Bangalore, Karnataka, India;* [2]*Department of Pathology, Kidwai Memorial Institute of Oncology, Bangalore, Karnataka, India and* [3]*Department of Biology, Indian Institute of Science Education and Research, Pune, Maharashtra, India*

Emerging evidence suggests that cancers arise in stem/progenitor cells. Yet, the requirements for transformation of these primitive cells remains poorly understood. In this study, we have exploited the 'mammosphere' system that selects for primitive mammary stem/progenitor cells to explore their potential and requirements for transformation. Introduction of Simian Virus 40 Early Region and hTERT into mammosphere-derived cells led to the generation of NBLE, an immortalized mammary epithelial cell line. The NBLEs largely comprised of bi-potent progenitors with long-term self-renewal and multi-lineage differentiation potential. Clonal and karyotype analyses revealed the existence of heterogeneous population within NBLEs with varied proliferation, differentiation and sphere-forming potential. Significantly, injection of NBLEs into immunocompromised mice resulted in the generation of invasive ductal adenocarcinomas. Further, these cells harbored a sub-population of $CD44^+/CD24^-$ fraction that alone had sphere- and tumor-initiating potential and resembled the breast cancer stem cell gene signature. Interestingly, prolonged *in vitro* culturing led to their further enrichment. The NBLE cells also showed increased expression of stemness and epithelial to mesenchymal transition markers, deregulated self-renewal pathways, activated DNA-damage response and cancer-associated chromosomal aberrations—all of which are likely to have contributed to their tumorigenic transformation. Thus, unlike previous *in vitro* transformation studies that used adherent, more differentiated human mammary epithelial cells our study demonstrates that the mammosphere-derived, less-differentiated cells undergo tumorigenic conversion with only two genetic elements, without requiring oncogenic Ras. Moreover, the striking phenotypic and molecular resemblance of the NBLE-generated tumors with naturally arising breast adenocarcinomas supports the notion of a primitive breast cell as the origin for this subtype of breast cancer. Finally, the NBLEs represent a heterogeneous population of cells with striking plasticity, capable of differentiation, self-renewal and tumorigenicity, thus offering a unique model system to study the molecular mechanisms involved with these processes.

Oncogene advance online publication, 29 August 2011; doi:10.1038/onc.2011.378

Keywords: adenocarcinoma; breast cancer stem cells; EMT; mammospheres; SV40ER; telomerase

Introduction

Recent studies have demonstrated the presence of stem cells in various adult human tissues including the breast. Additionally, several cancers, such as, leukemia, glioma, breast carcinoma and others have been shown to harbor a rare population of cells termed 'cancer stem cells' (CSCs) that appear to be critical for tumor growth and maintenance (Tan *et al*., 2006). The hierarchical organization of cancers and the phenotypic and functional resemblance between normal and CSCs has led to the speculation that cancers arise in normal, tissue-specific stem/progenitor cells (Pardal *et al*., 2003; Phesse and Clarke, 2009; Rodriguez Salas *et al*., 2010; Shackleton, 2010). Yet, the perturbations required for the tumorigenic transformation of these primitive cells remains unknown. Given the striking parallels between normal stem cells and cancer cells, including extensive self-renewal, expression of telomerase and ability to grow in anchorage-independent conditions (Liu *et al*., 2005), it is possible that these immature cells require fewer alterations for transformation compared with their more differentiated counterparts that lack these properties.

Stem cells within the mammary gland have been identified using electron microscopic studies and cell surface markers (Woodward *et al*., 2005). More recently, a small sub-population of human mammary epithelial cells (HMECs) was shown to form three-dimensional (3D) spheroids called mammospheres when grown in suspension *in vitro* (Dontu *et al*., 2003). Mammospheres are largely comprised of primitive mammary stem and progenitor cells of varying proliferation potential, and capable of undergoing both self-renewal and multilineage differentiation *in vitro* (Dontu *et al*., 2003). Moreover, transplantation of mammospheres into cleared mammary fat pad generated complete

Correspondence: Dr A Rangarajan, Department of Molecular Reproduction, Development and Genetics, Indian Institute of Science, CV Raman Avenue, Karnataka, Bangalore 560012, India.
E-mail: anu@mrdg.iisc.ernet.in
Received 20 February 2010; revised 21 June 2011; accepted 24 July 2011

mammary structures *in vivo*, further confirming the presence of long-term self-renewing stem/progenitor population within mammospheres (Liao *et al*., 2007). Thus, unlike HMECs grown in adherent conditions that promote differentiation (Muschler *et al*., 1999), growth in suspension appears to enrich for mammary stem and progenitor cells.

In vitro manipulation of HMECs has served as a useful strategy to understand the molecular mechanisms of breast cell transformation (Dimri *et al*., 2005). For example, introduction of HPV E6 and E7 into primary HMECs led to their immortalization (Wazer *et al*., 1995; Gudjonsson *et al*., 2002). In another study, introduction of Simian Virus 40 Early Region (SV40ER) and the catalytic subunit of human telomerase (hTERT) into adherent HMECs led to the generation of immortalized HMLE cells (Elenbaas *et al*., 2001). More recently, introduction of hTERT-alone was shown to suffice for the immortalization of HMECs grown in a specialized media (Zhao *et al*., 2010). Tumorigenic transformation required additional activation of strong oncogenic signaling. For example, overexpression of oncogenic Ras resulted in the transformation of HMLE cells, leading to the generation of squamous cell carcinoma (Elenbaas *et al*., 2001). In yet another study, HMECs grown in a specialized media called WIT and carrying SV40ER, hTERT and oncogenic Ras led to the generation of adenocarcinomas (Ince *et al*., 2007). However, both these latter models required supra-physiologic expression of oncogenic Ras, while mutations in the Ras oncogene are very rare in breast cancers (Rochlitz *et al*., 1989). In another study, mere activation of Wnt signaling in adherent HMECs enabled transformation of a subtype of breast cells that generated medullary carcinoma (Ayyanan *et al*., 2006). Taken together, these various studies indicate that the combination of cell type of origin and the nature of initiating oncogenes likely determines the requirement and the phenotype of the resultant tumor.

In this study, we show that the overexpression of SV40ER and hTERT into mammosphere-derived, primitive breast cells sufficed for their tumorigenic transformation. The resultant NBLE cells retained stem-like properties, contained a sub-population resembling breast CSCs and generated invasive breast adenocarcinomas, the most common type of human breast cancers encountered in the clinic. Furthermore, gene expression profiling revealed a close resemblance with naturally arising tumors. Thus, our study provides a novel breast cancer model system to begin to understand the molecular mechanisms involved in the transformation of primitive breast cells with stem-like properties.

Results

Establishment of immortalized mammosphere-generating breast cell line that retains stemness properties

Mammospheres growing in suspension are enriched in mammary stem and progenitor cells (Dontu *et al*., 2003). In keeping with this, a reverse transcriptase–PCR (RT–PCR) analysis comparing HMECs grown as monolayers versus mammospheres revealed an increased expression of stemness-related genes (such as, *Bmi1*, *Nanog*, *Lef1*, *Gli1*, *Notch1*, *Hes1*, *HeyL* and *CD44*), and epithelial to mesenchymal transition (EMT) markers associated with stemness (such as, Vimentin, N-cadherin, FN1, Snai1 and Slug1) (Mani *et al*., 2008) in mammospheres (Figure 1a). We had previously demonstrated that the lifespan of normal mammospheres *in vitro* is limited to four passages (Dey *et al*., 2009), thereby limiting their utility for studying mammary stem cell biology. Therefore, we sought to generate immortalized breast cell lines that retain long-term stem-like properties. To do so, we transduced single cells obtained from primary T1 mammospheres (derived from normal breast tissue NB130) with pCSCG lentiviruses carrying SV40ER (that encodes for LT and ST) and hTERT, alone, and in combination, and grew these transduced cells in adherent as well as suspension conditions parallelly. Overexpression of LT antigen and hTERT was confirmed by immunoblotting and RT–PCR analysis, respectively (Supplementary Figure S2a). In adherent condition, the untransduced parental cells and those transduced with hTERT-alone proliferated for $\sim$20 population doublings (Figure 1b) before senescing

Figure 1 Establishment of NBLE breast cell line with long-term stemness properties. (**a**) Graph shows fold change in gene expression (normalized to HPRT) of HMECs grown in suspension over attachment for a week ($n=3$). (**b**) Growth curves of parental NB130 cells and those transduced with the indicated genetic elements and grown in adherent culture conditions. The *y* axis represents population doublings post-transduction. (**c**) Graph represents the number of passages in suspension of parental NB130-derived mammospheres and those transduced with the indicated genetic elements. Mammospheres were trypsinized every seventh day, which was considered as one passage. Inset shows phase-contrast (PC) and fluorescence (FS) images of green fluorescent protein (GFP)-positive NBLE cells grown in attachment (Att) and suspension (Sus) conditions (scale bar: 50 μm). (**d**) Graph shows sphere-forming efficiency for indicated cell types ($n=3$), error bars indicate s.d. (**e**) Graph shows fold change in gene expression (normalized to HPRT) of indicated genes between NBLE cells grown in attachment over suspension for a week ($n=3$), error bars indicate s.d. (**f**) Graph shows expression of differentiation markers in NBLE cells grown in non-serum containing regular growth media (gray bars) and serum-containing, differentiation-inducing media (black bars) as analyzed by immunofluorescence staining. *Y* axis represents mean fluorescence intensity (AU, arbitrary units) of 20 randomly chosen cells measured using ImageJ software (NIH, Bethesda, MD, USA) ($n=3$), error bars indicate s.d., *P*-value was calculated with paired *t*-test (*** indicates *P*-value <0.001). (**g**) Graph shows percentage of acinar and tree structures formed by individual NBLE cells seeded at limiting dilutions (100 cells/well of a 96-well plate) in matrigel for 12–14 days ($n=5$), error bars indicate s.d. Inset shows images of a CK18-positive acinus (top panel; nuclei counterstained with Hoechst-33342) and a tree-structure (bottom panel) (scale bar: 50 μm). (**h**) Graph represents percentage of CK18-positive pure luminal colonies (Lum), CK14-positive pure myoepithelial colonies (Myo) and the mixed type colonies largely containing dual-positive cells (Mixed) generated by NBLE cells grown at clonal densities (500 cells/ml) in differentiation-inducing conditions ($n=3$). Inset shows representative colony of each type (nuclei counterstained with Hoechst-33342, scale bar: 50 μm).

(Supplementary Figure S2b), whereas SV40ER-expressing cells divided further before undergoing cell death. The cells expressing both SV40ER and hTERT continued to proliferate beyond 50 population doublings (Figure 1b). In suspension, the un-transduced parental cells and those transduced with empty vector or hTERT-alone failed to generate mammospheres beyond five passages (Figure 1c). Cells transduced with SV40ER-alone grew past T5 but underwent large-scale cell death after T8 and failed to generate any more mammospheres. However, those carrying both SV40ER and hTERT continued to generate spheres beyond eight passages (~100 population doublings), indicating that they are immortalized. We have termed these as NBLE cells (Figure 1c—inset). Similar results were obtained for two other independently transduced primary mammospheres (derived from NB74 and NNB1; Supplementary Figures S2c and S2d).

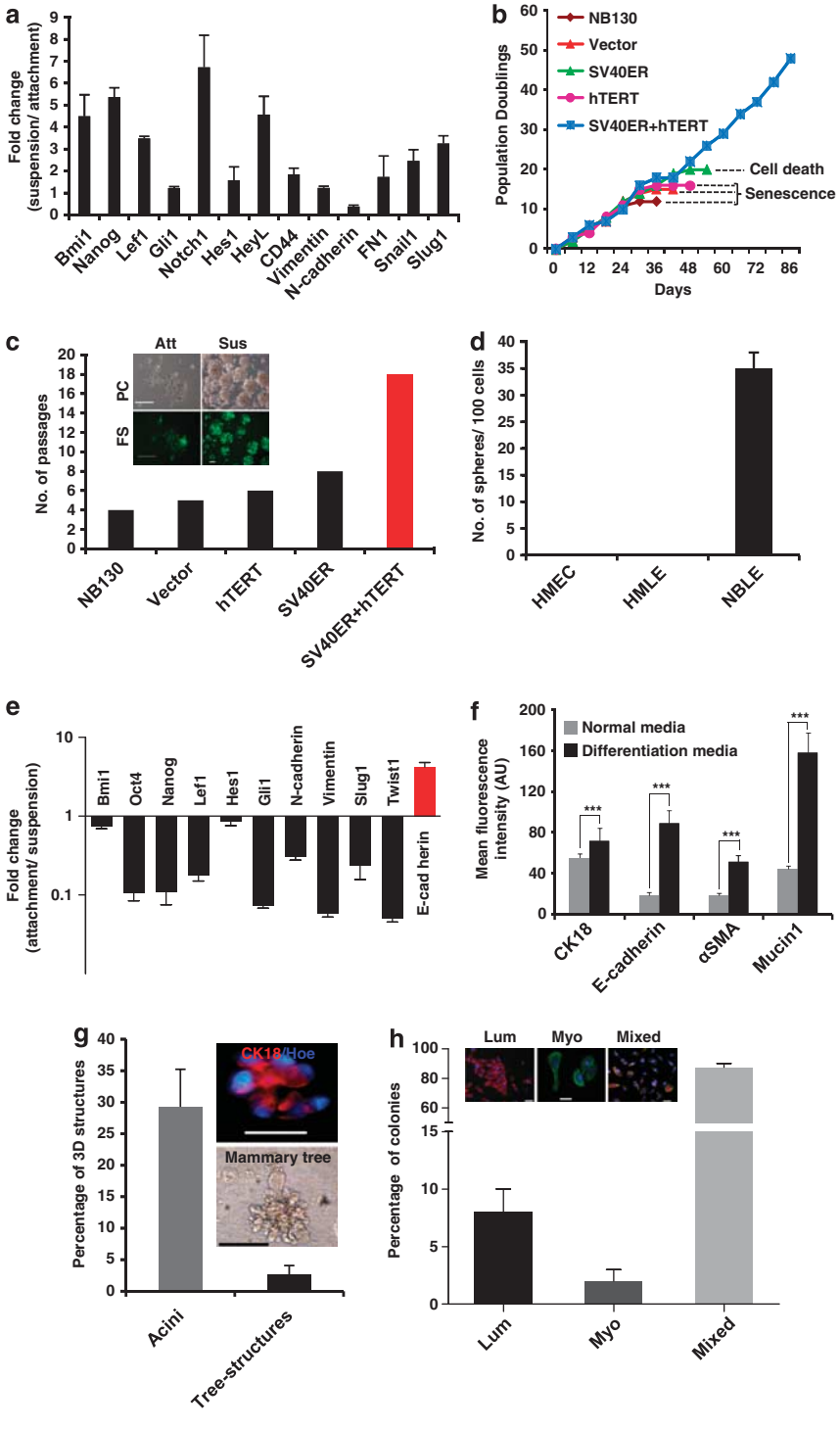

We further characterized the stemness and differentiation properties of the immortalized NBLE cells. These cells generated spheres at a high frequency of ~35% when seeded at limiting dilutions of one cell per well, whereas primary HMECs and immortalized HMLEs failed to form any spheres under these conditions (Figure 1d). Further, the NBLE cells retained the expression of stemness markers similar to primary mammospheres (Supplementary Figure S2e). Another independently immortalized mammosphere-derived cell line (NB74LE) also showed retention of stemness markers (Supplementary Table S2). When seeded in adherent condition, the NBLE cells attached within 6–8 h, and after 4 days of growth in attachment, they showed reduction in expression of stemness and EMT markers and increase in the expression of E-cadherin (Figure 1e) revealing that attachment promoted differentiation. Interestingly, NBLE cells could be propagated in adherent conditions while retaining the ability to form spheres when subjected to suspension (Figure 1c—inset). Thus, the NBLE cells provide a unique reversible model for studying the switch between differentiation and stemness.

To assess if the NBLE cells are also capable of undergoing differentiation, they were cultured in differentiation-inducing media in attachment (see Materials and methods section). Under these conditions, NBLE cells showed elevated expression of epithelial differentiation markers such as, CK18, E-cadherin, αSMA and Mucin1 (Figure 1f) and an increase in the number of CK14-positive cells (Supplementary Figures S3a and S3b). Further, when grown in matrigel, which provides physiological cues that allows for mammary morphogenesis (Bissell *et al*., 1999), individual NBLE cells formed 3D acini staining positive for CK18 and branched tree structures (Figure 1g). Together, these data showed that in addition to stemness, the NBLE cells also retained the ability to differentiate.

To better understand the cellular composition of NBLE cells, they were cultured at clonal densities (500 cells/ml) in adherent, differentiating conditions. Three types of colonies were observed after 8–10 days: (1) <10% CK18-positive pure luminal colonies, (2) <5% CK14-positive pure myoepithelial colonies and (3) >85% of mixed colonies comprising largely of dual-positive cells in addition to some cells positive only for CK14 or CK18 (Figure 1h and inset), revealing the presence of a large number of bi-potent progenitors within NBLE cells. We further derived nine single cell clones of NBLE cells and assessed for various properties such as morphology, proliferation, sphere-forming efficiency, expression of epithelial and mesenchymal markers, progenitor-content, *in vitro* differentiation-potential, stemness/EMT markers and CD44 expression as shown in (Figures 2a–f, Supplementary Figures S4a and S4b). Based on morphology, these clones could be broadly classified as epithelial-like (clones E6 and E7), mesenchymal (clones C4, C8 and F4) and intermediate (clones B7, D7, E5 and E10) clones. The epithelial clones showed lower proliferation rate, poor sphere forming efficiency, higher expression of E-cadherin, contained uni-potent cells positive for CK14 and failed to generate 3D structures in matrigel. In contrast, the mesenchymal clones had higher proliferation rate, formed spheres at very high efficiency, expressed low E-cadherin and high Vimentin, consisted of bi-potent progenitors positive for both CK14 and CK18, and generated very large but poorly organized 3D tree structures in matrigel. The intermediate clones proliferated moderately, showed variable sphere forming efficiency, expressed very low E-cadherin, contained uni- and bi-potent progenitors and formed small 3D structures in matrigel (Supplementary Table S3).

Taken together, these experiments revealed that the introduction of SV40ER and hTERT into mammosphere-derived cells led to their immortalization with retention of stemness properties. Further, the resultant NBLE cells represent a heterogeneous population with varied proliferation, differentiation, self-renewal and other stem-like properties.

NBLE cells generate invasive ductal adenocarcinomas in immunocompromised mice

Since NBLE cells were immortal, showed long-term self-renewal *in vitro* and ability to grow in anchorage-independent conditions—properties typically associated with cancerous cells—we checked for their tumorigenic potential *in vivo*. The NBLE cells injected subcutaneously into immunocompromised mice gave rise to well-vascularized, poorly differentiated, highly invasive tumors in 6 weeks (Figures 3a and d—inset), whereas primary mammosphere-derived cells failed to initiate tumors even after 3 months. Similar results were obtained with yet another independently derived immortalized mammosphere cell line NB74LE (Figure 3a). Expression of green fluorescent protein and LT antigen by the tumor-derived cells (Figure 3b), and detection of LT antigen in tumor sections (Figure 3c) confirmed that the tumors were indeed formed by NBLE cells. Further histopathological analysis of the tumors revealed that

Figure 2 Single cell clonal analysis reveals heterogeneous population within NBLEs. NBLE cells were seeded at 1 cell per well dilution in a 96-well plate and single cells, confirmed microscopically, were expanded sequentially. All experiments were performed within two to three passages. (**a**) Phase-contrast images of various clones (scale bar: 50 μm). (**b**) Graph represents proliferation of NBLE-clones with values representing average of two experiments. (**c**) Graph shows the number of mammospheres (>100 μm) formed by cells from NBLE clones seeded as 100 cells/well of a 96-well plate ($n=3$), error bars indicate s.d. (**d**) Representative pictures of immunofluorescence staining of different clones for epithelial markers (E-cadherin, αSMA and Mucin1) and mesenchymal marker (Vimentin) ($n=2$, nuclei counterstained with Hoechst-33342 and pseudocolored red, scale bar: 50 μm). (**e**) The images represent NBLE clones dual-stained for CK14 (red) and CK18 (green) ($n=2$, nuclei counterstained with Hoechst-33342 and pseudocolored blue, scale bar: 50 μm). (**f**) Phase-contrast images show 3D structures formed by NBLE clones in matrigel ($n=2$, scale bar: 50 μm).

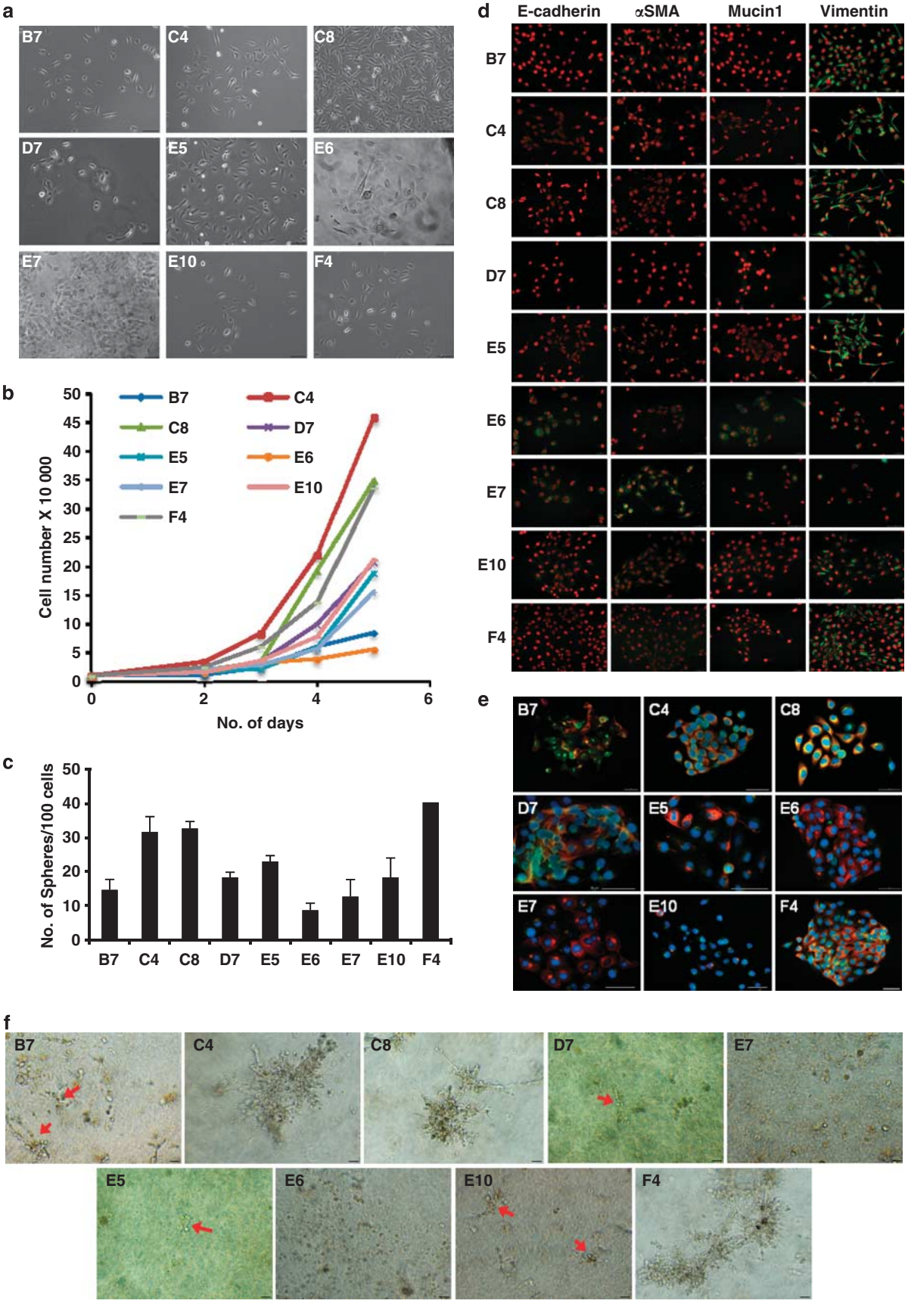
a
B7
C4
C8
D7
E5
E6
E7
E10
F4
b
Cell number X 10 000
No. of days
B7
C4
C8
D7
E5
E6
E7
E10
F4
c
No. of Spheres/100 cells
B7
C4
C8
D7
E5
E6
E7
E10
F4
d
E-cadherin
αSMA
Mucin1
Vimentin
e
f

a

Cell type injected	Cell Number	Tumors/ Injections
Primary mammospheres	$2X10^6$	0/4
NBLE	$1X10^6$	4/4
NB74LE	$2X10^6$	6/6

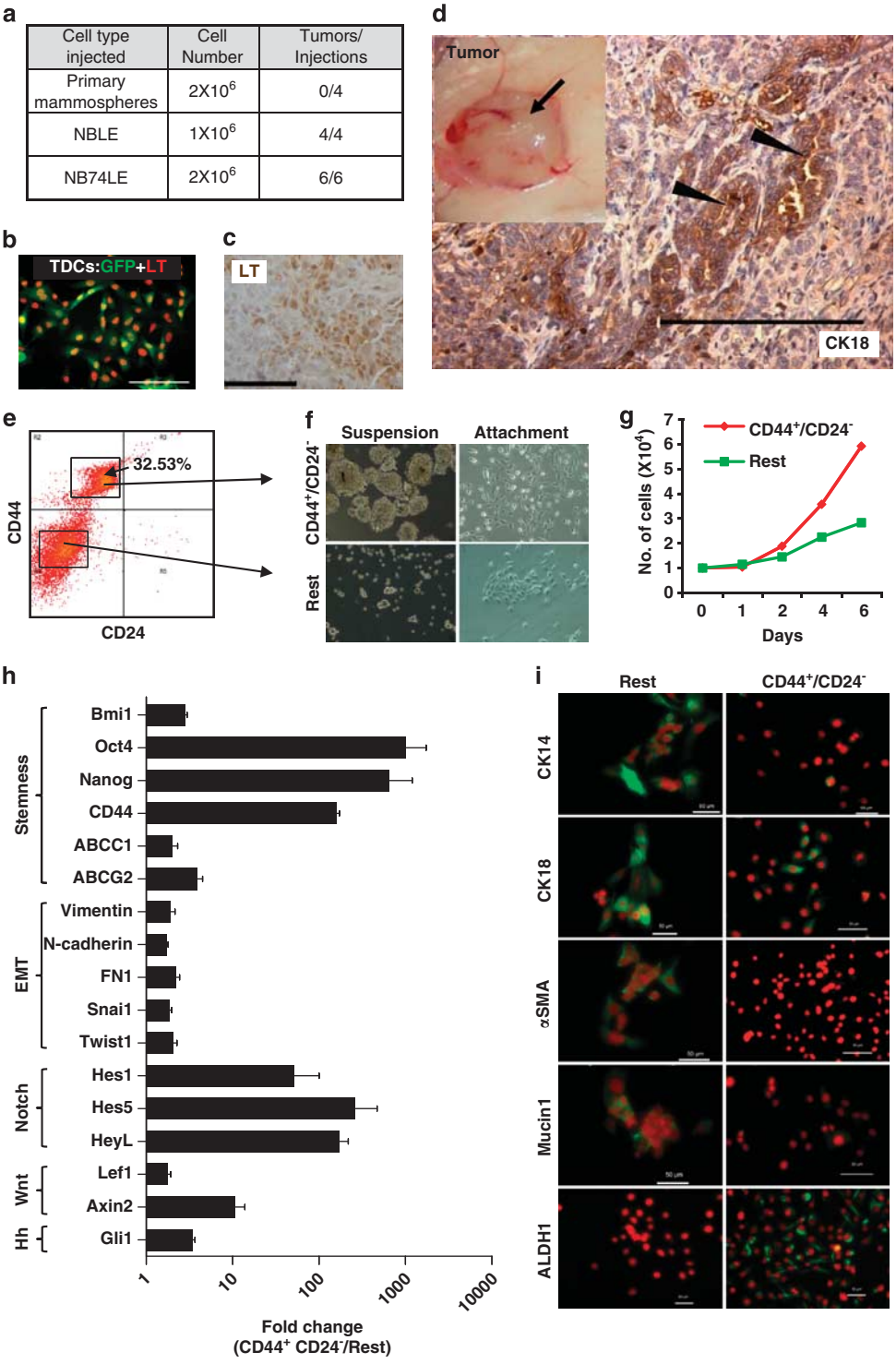

Figure 3 NBLE cells generate adenocarcinomas and harbor $CD44^+/CD24^-$ fraction resembling CSCs. (**a**) Chart shows the *in vivo* tumor formation data for primary mammosphere-derived cells, NBLEs and NB74LE cells. (**b**) Image shows expression of green fluorescent protein (GFP) (green) and LT (red) in NBLE tumor-derived cells ($n=2$, scale bar: 50 μm). (**c**) Image shows tumor section stained for LT ($n=2$, scale bar: 50 μm). (**d**) Immunohistochemical analysis of NBLE tumor section for CK18 expression (arrowheads show CK18-positive cells lining the ducts) ($n=3$, scale bar: 100 μm, inset shows highly vascularized tumor). (**e**) Representative plot showing two color flow cytometry analysis for CD44 and CD24 expression in NBLE cells ($n=3$). (**f**) Phase-contrast images show sorted $CD44^+/CD24^-$ and 'rest' fractions of NBLE cells seeded for a week in suspension (left panels) and in attachment (right panels) ($n=3$). (**g**) Graph shows growth curves of sorted $CD44^+/CD24^-$ and 'rest' fractions of NBLE cells seeded in attachment culture with values representing average of two experiments. (**h**) Graph shows fold change in gene expression (normalized to HPRT) of $CD44^+/CD24^-$ fraction over 'rest' fraction of NBLE cells ($n=3$), error bars indicate s.d. (**i**) Images show immunocytochemical analysis of sorted 'rest' and $CD44^+/CD24^-$ fractions of NBLE cells stained for epithelial and stemness markers ($n=3$, nuclei counterstained with Hoechst-33342 and pseudocolored red, scale bar: 50 μm).

they largely comprised epithelial ductal structures that were CK18-positive (Figure 3d), a characteristic of ductal adenocarcinomas (Chu and Weiss, 2002). In addition, very few keratin pearls, characteristic of squamous cell carcinomas, were also detected (Supplementary Figure S5). Immunohistochemical analysis further revealed that these tumors were negative for ER, PR and HER2-Neu (data not shown), thereby resembling the triple-negative tumors that represent one of the most aggressive types of breast cancers. Thus, these data indicated that the introduction of SV40ER and hTERT sufficed for the tumorigenic conversion of primary mammosphere-derived cells.

NBLEs harbor a sub-population of CD44$^+$/CD24$^-$ cells, which exhibits CSC properties

Recent studies have demonstrated that the CD44$^+$/CD24$^-$ marker profile represents the sub-population of breast cancer cells termed 'CSCs' (Al-Hajj *et al*., 2003; Ponti *et al*., 2006). Flow cytometry analysis revealed that the NBLEs harbored $\sim$32% of CD44$^+$/CD24$^-$ cells (Figure 3e). When the sorted CD44$^+$/CD24$^-$ and the 'rest' fractions of NBLE cells were seeded in suspension at a low density of 1000 cells/ml, only the CD44$^+$/CD24$^-$ fraction formed spheres (Figure 3f, left panels). When grown under adherent condition the CD44$^+$/CD24$^-$ fraction appeared more mesenchymal (Figure 3f, right panels) and showed higher proliferation rate (Figure 3g) compared with the 'rest' fraction. Further RT–PCR analysis revealed that compared with the 'rest' fraction, the CD44$^+$/CD24$^-$ fraction of NBLE cells expressed increased stemness and EMT-related genes, such as *Bmi1*, *Oct4*, *Nanog*, *CD44*, *ABCC1*, *ABCG2*, *Vimentin*, *N-cadherin*, *FN1*, *Snai1* and *Twist1* (Figure 3h). Additionally, this fraction showed increased activation of self-renewal pathways such as the Notch, Wnt and Hedgehog, as revealed by the increased expression of their downstream targets (Figure 3h). Immunocytochemical analysis further showed that the CD44$^+$/CD24$^-$ fraction exhibited reduced epithelial markers (CK14, CK18, αSMA and Mucin1) and increased ALDH1 expression compared with the 'rest' fraction (Figure 3i and Supplementary Figure S6). Thus, the CD44$^+$/CD24$^-$ fraction of NBLE cells showed several characteristics of breast CSCs (Charafe-Jauffret *et al*., 2009).

To further address if the CD44$^+$/CD24$^-$ fraction of NBLE cells resembled CSCs from naturally occurring cancers, we undertook genome-wide microarray analysis comparing the gene expression of CD44$^+$/CD24$^-$ versus the 'rest' fraction of NBLE cells with that of three primary invasive grade III ductal adenocarcinoma samples (CB272, CB361 and CB386) and a published gene signature of microarray analysis on tumor-initiating cells from 13 primary breast cancer samples (Creighton *et al*., 2009). Unsupervised hierarchical clustering of significantly regulated genes (fold change >1.2, $P<0.05$) from NBLE showed striking similarities with the primary cancer samples (Figure 4a, Supplementary Figures S7, S8 and Supplementary Tables S4, S5) as well as with the published literature (Supplementary Figure S9a and Supplementary Table S6). Consistent with the RT–PCR data (Figure 3h), and previous reports (Liu *et al*., 2005; O'Brien *et al*., 2010), the gene expression profile of NBLE-CD44$^+$/CD24$^-$ fraction showed deregulation of self-renewal pathways including Notch, Wnt, Hedgehog and transforming growth factor-β (Supplementary Figure S9b and Supplementary Table S7). The NBLE gene expression pattern also showed similarities with various genes involved in the regulation of embryonic stem cells (Supplementary Figure S9b and Supplementary Table S7) consistent with earlier reports (Ben-Porath *et al*., 2008). Additionally, when we injected the sorted sub-fractions of NBLE cells into NOD/SCID mice, only the CD44$^+$/CD24$^-$ fraction gave rise to tumors within 4 weeks whereas the 'rest' fraction failed to do so even after 10 weeks (Figure 4b). Taken together, all these observations clearly showed that the CD44$^+$/CD24$^-$ fraction of NBLE cells showed close resemblance with that of tumorigenic breast CSCs, thus making NBLE a suitable and renewable system for exploring the biology of CSCs.

Interestingly, prolonged *in vitro* culturing of NBLE cells for $\sim$35 passages resulted in late passage cells (henceforth referred to as NBLE-LP) that showed mesenchymal morphology (Figure 4c) and exhibited increased expression of stemness and EMT markers and decreased epithelial markers compared with NBLE cells (Figure 4d and Supplementary Figures S10a and S10b). Further, flow cytometry analysis revealed that the NBLE-LP cells harbored almost 96% of CD44$^+$/CD24$^-$ cells (Figure 4e) compared with 32% in NBLE (Figure 3e). Consistent with this, the NBLE-LP cells generated tumors (Figure 4b) at a much faster rate compared with NBLE cells (data not shown). These data revealed that *in vitro* passaging of NBLE cells led to the selection and expansion of a sub-population of cells with breast CSC properties.

Karyotyping reveals heterogeneous chromosomal aberrations in NBLE cells

To further understand the heterogeneity and plasticity of NBLE cells, we undertook detailed karyotyping (Figures 5a and b). In accordance with previous SV40ER-based transformation models (Woods *et al*., 1994; Elenbaas *et al*., 2001), we detected several chromosomal aberrations including chromosomal gains (+), losses (−), breaks, deletions, translocations and derivative chromosomes in NBLE cells. Analyses of eight different metaphase-spreads from NBLE cells showed a heterogeneous karyotype with chromosome numbers ranging from 51 to 63. These cells showed chromosomal aberrations that included gains of Chr. 3?, 5, 6, 6q25, 12, 13p11, 14, 15?, 15p11, 17?, 20 and 21p11, and losses of Chr. 1, 2, 3?, 4, 7, 8, 10, 11, 13, 15?, 16, 17?, 18, 19, 21, 22 and X as shown in Figure 5a together suggestive of the presence of multiple transformed clones within NBLE cells. Further, karyotyping of NBLE late passage cells (NBLE-LP) derived by long-term

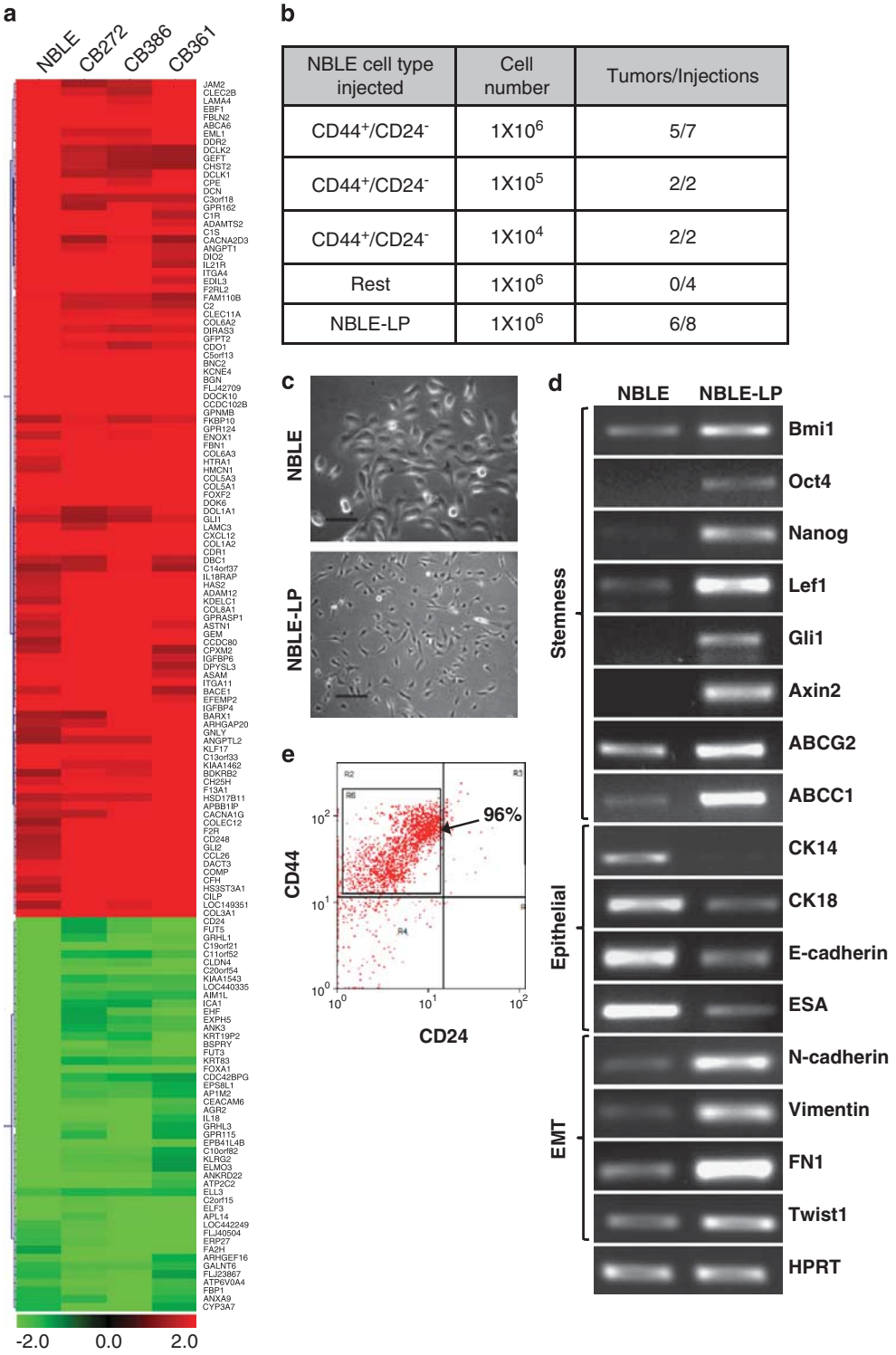

NBLE cell type injected	Cell number	Tumors/Injections
$CD44^+/CD24^-$	$1X10^6$	5/7
$CD44^+/CD24^-$	$1X10^5$	2/2
$CD44^+/CD24^-$	$1X10^4$	2/2
Rest	$1X10^6$	0/4
NBLE-LP	$1X10^6$	6/8

Figure 4 Gene expression profiling shows similarities with breast cancer stem-like cells. All microarray data represent competitive hybridizations undertaken between sorted $CD44^+/CD24^-$ and 'rest' fractions. The heat map shows the fold changes of significantly altered gene expression (>1.2 fold, $P<0.05$) of the $CD44^+/CD24^-$ fraction over the 'rest' fractions with red indicating high, black showing no-change, and green depicting low levels of expression. (**a**) Comparison of gene expression pattern of NBLE with grade III primary invasive ductal adenocarcinoma samples CB272, CB386 and CB361 (see gene list in Supplementary Table S5). (**b**) Chart shows *in vivo* tumor formation data for $CD44^+/CD24^-$ and 'rest' fractions of NBLE cells and NBLE-LP cells. (**c**) Phase-contrast images show the morphology of NBLE and NBLE-LP cells obtained by long-term *in vitro* passaging of NBLEs in adherent condition ($n=2$, scale bar-50 μm). (**d**) Representative RT–PCR data comparing gene expression between NBLE and NBLE-LP cells. (**e**) Representative plot showing two color flow cytometry analysis for CD44 and CD24 expression in NBLE-LP cells ($n=3$).

a

Sl.#	Modal Number	Chr. 1	2	3	4	5	6	7	8	9	10	11	12	13
1	63 XXX (3n)	-1	-1	0	0	+1	+1 add6q25	-1	0	0	-1	-1	0	-1 t(13;13)
2	60 XX (3n)	-1	-1	-1	0	0	+1 add6q25	0	-1	0	-1	-1	0	-1 add13p11
3	59 XX (3n)	-1	-1	0	0	+1	0 add6q25	-1	0	0	-1	-1	+1	-1 add13p11
4	57 XX (2n)	0	0	+1	+1	+2	0 add6q25	0	0	+1	-1	0	+1	0 add13p11
5	63 XXX (3n)	-1	-1	0	0	+1	0 add6q25	-1	0	-1	-2	0	0	-1 add13p11
6	51 X (2n)	0	-1	+1	-1	+1	0 +add6q25	-1	+1	0	0	0	0	+1 add13p11
7	59 XXX (3n)	-1	0	-2	-1	0	+1 +add6q25	-1	-1	0	-1	-1	-1	-1 add13p11
8	60 XX (3n)	-1	-1	0	0	+1	0 +add6q25	-1	0	0	-1	-1	0	0 [add13p11]2
	% aberrations	75	75	50	37.5	75	100	75	37.5	25	87.5	62.5	37.5	100

Sl.#	Modal Number	14	15	16	17	18	19	20	21	22	X	Y	Mar
1	63 XXX (3n)	+1	+1 add15p11	-1	0	0	-1	0	-1 add21p11	0	0	0	0
2	60 XX (3n)	0	0 add15p11	-1	-2	0	-1	0	-1	0	-1	0	+3
3	59 XX (3n)	+1	-1 add15p11	-1	-1	-1	0	0	-1	-1	-1	0	0
4	57 XX (2n)	+2	+1	0	+1	+1	0	+1	0 add21p11	0	0	0	0
5	63 XXX (3n)	+2 add14p11	-1	0	0	0	-1	-1	-2	+1	+1 BRK	0	+1
6	51 X (2n)	+1	+1 add15p11	-1	+1	0	0	+2	0 add21p11	0	-1	0	+1
7	59 XXX (3n)	-1	0 add15p11	-2	-1	0	-1	+1	0	-1	0	0	+4
8	60 XX (3n)	0	-1	-1	0	-1	-1	0	0 add21p11	0	-1	0	0
	% aberrations	75	100	75	62.5	37.5	62.5	50	87.5	37.5	62.5	NA	NA

Gain | Loss | No change

b

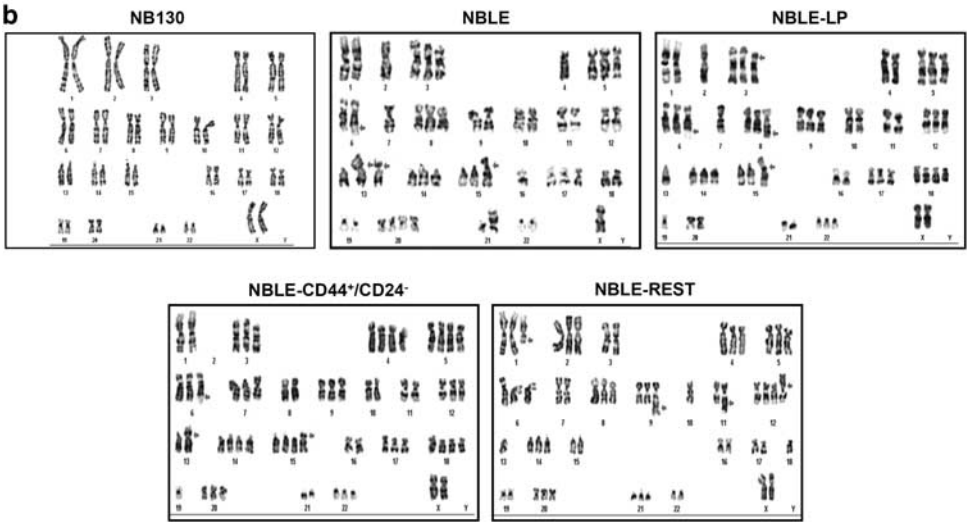

Figure 5 Karyotyping reveals heterogeneous chromosomal abnormalities in NBLE cells. (**a**) Chart shows aberrations in various chromosomes in eight different NBLE cells. Dark grey represents loss of chromosome, light grey represents gain of chromosome and white represents no change. (**b**) Images show single representative karyotype for parental NB130, NBLE and its derivatives.

in vitro culturing of NBLEs showed a reduction in chromosome numbers from near-triploid (59) to a hyper-diploid (53) state. Additionally, the NBLE-LP cells showed unique aberrations such as gains of Chr. 3p21, 4, 7, 8, 8q24, 9, 13, 18, 19, 22 and Xp21 (Supplementary Table S8), together revealing that the NBLE cells are in a plastic state. Interestingly, the tumorigenic $CD44^+/CD24^-$ fraction and non-tumorigenic 'rest' fraction of NBLEs showed unique aberrations. The $CD44^+/CD24^-$ fraction showed whole chromosome losses of Chr. 1, 2, 8, 11, 16, 19, 20, 21 and X and gains in Chr. 6q25, 13p11 and 15p11, whereas the 'rest' population showed a comparatively reduced frequency of chromosome losses (primarily of Chr. 1q24, 13) while chromosomal gains of Chr. 1, 4, 9q34, 11p13, 12, 12p12, 17, 17p12, 19?, 20 and 21 were noted (Supplementary Table S8), suggesting that these differences may have contributed to the tumorigenicity of the $CD44^+/CD24^-$ fraction. Taken together, these data revealed the presence of multiple clones within NBLE population that are under continuous selection, which may, in part explain the plasticity exhibited by these cells with respect to differentiation, self-renewal and tumorigenicity.

We next gauged for possible molecular mechanisms that may have additionally contributed to the tumorigenicity of NBLE cells. Gene expression profiling of NBLE cells revealed increased expression of several genes that induce EMT whereas the genes that suppress EMT were significantly downregulated (Figure 6a and Supplementary Table S9). RT–PCR analysis additionally

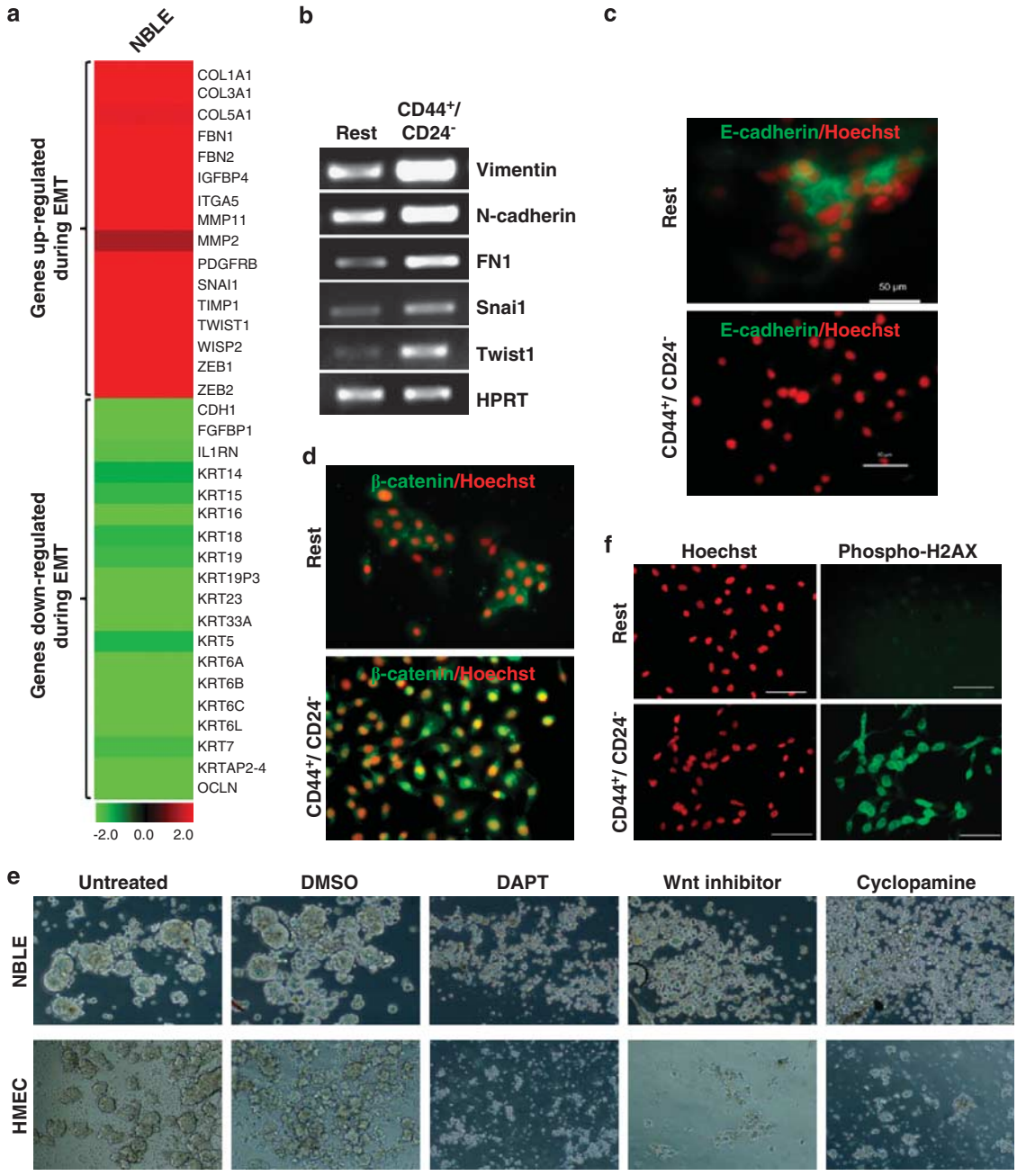

Figure 6 Molecular mechanisms associated with tumorigenic conversion of NBLE cells. (**a**) Heat map shows the status of EMT-related genes in the microarray analyses comparing the sorted $CD44^+/CD24^-$ versus 'rest' fraction of NBLE cells. (**b**) Representative RT–PCR data showing expression of EMT markers in the sorted $CD44^+/CD24^-$ and 'rest' fractions of NBLE cells ($n=5$). Images show expression of E-cadherin (**c**) and β-catenin (**d**) in 'rest' and $CD44^+/CD24^-$ fractions of NBLE cells as detected by immunocytochemical analysis ($n=3$, nuclei counterstained with Hoechst-33342 and pseudo-colored red). (**e**) Phase-contrast images show the effect of DAPT, Wnt inhibitor and Cyclopamine (inhibitors of Notch, Wnt and Hedgehog pathways, respectively) on mammosphere formation by NBLE cells (upper panel) and primary HMECs (lower panels). Untreated, and vehicle (dimethylsulphoxide (DMSO)) treatment served as controls ($n=3$). (**f**) Images show phospho-H2AX expression in 'rest' and $CD44^+/CD24^-$ fractions of NBLE cells ($n=2$, nuclei counterstained with Hoechst-33342 and pseudocolored red, scale bar: 50 μm).

confirmed that genes related to induction of EMT were upregulated in the $CD44^+/CD24^-$ fraction (Figure 6b). Immunocytochemical analysis revealed complete loss of E-cadherin in the $CD44^+/CD24^-$ fraction of NBLE cells (Figure 6c) with corresponding nuclear localization of β-catenin (Figure 6d). Concurrent to our RT–PCR and microarray results, which showed activation of self-renewal pathways (Figure 4d and Supplementary Figures S10a and S10b), when we inhibited the Notch, Wnt and Hedgehog pathways individually using pharmacological inhibitors the sphere-forming efficiency of NBLE cells was completely abrogated similar to primary HMECs in suspension (Figure 6e). Additionally, while almost all the tumorigenic $CD44^+/CD24^-$

fraction of NBLE cells showed elevated phospho-H2AX, a marker of DNA-damage response, the 'rest' fraction failed to show any (Figure 6f). Thus, the induction of EMT, deregulation of self-renewal pathways and activation of DNA-damage response are some of the likely mechanisms to have contributed to the tumorigenic conversion of mammospheres with the acquisition of cancer stem-like properties.

Discussion

Starting from mammospheres that are enriched in primitive breast stem/progenitor cells, we demonstrate that the introduction of two genetic elements, SV40ER and hTERT, suffices for their tumorigenic conversion with the generation of breast cancer stem-like cells (Figure 7). Furthermore, the phenotypic and molecular resemblance of the mammosphere-derived transformed cells with invasive ductal adenocarcinomas, the most common type of breast cancers encountered in the oncology clinic, supports the notion of a stem/progenitor origin for these cancers.

We previously reported that normal mammospheres can be passaged in suspension for a maximum of four passages, beyond which they fail to generate spheres and largely undergo senescence (Dey *et al*., 2009). On the other hand, immortalized mammary cell line such as HMLEs (Elenbaas *et al*., 2001) can be cultured *in vitro* for prolonged periods; however, they lack the ability to generate mammospheres (Mani *et al*., 2008; Morel *et al*., 2008), indicating the lack of stem-like properties. In this study, we have demonstrated the successful generation of a breast cell line, NBLE, which can be continuously propagated *in vitro* without losing stem-like properties. Detailed cytogenetic and clonal analyses additionally revealed the presence of multiple clones with varied potential for proliferation, differentiation and self-renewal. Most significantly, these cells harbored a sub-population of $CD44^+/CD24^-$ cells that resembled the breast CSCs, and generated adenocarcinomas in immunocompromised mice. Thus, the plasticity exhibited by the NBLE cells with respect to differentiation, self-renewal and tumorigenicity makes them a unique model system to further decipher the mechanisms involved with these processes.

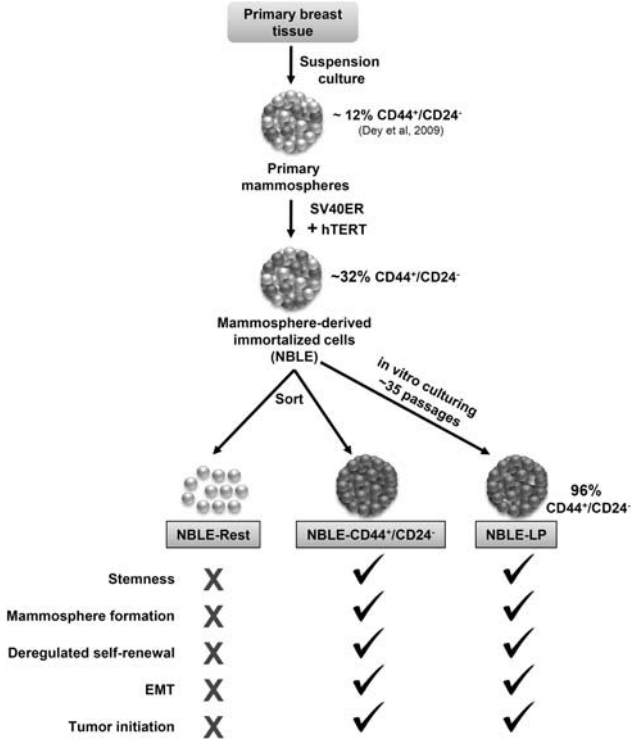

Figure 7 Schematic showing the generation and characteristics of tumorigenic NBLE cells.

Previous studies involving *in vitro* transformation of HMECs have led to the establishment of model systems to study different types of breast cancers. The HMLERs derived from adherent HMECs generated squamous cell carcinomas (Elenbaas *et al*., 2001), which represent $<5\%$ of naturally occurring breast cancers. The BPLERs derived from HMECs cultivated in specialized media called WIT generated malignant adenocarcinomas (Ince *et al*., 2007); however, both these models showed an absolute requirement for oncogenic Ras for transformation, while Ras mutations are found in $<5\%$ of naturally arising breast cancers. The Wnt-transformed HMECs generated medullary breast carcinomas (Ayyanan *et al*., 2006), which represent 2% of all breast tumors. In contrast, the NBLE cells reported in this study generated invasive tumors, which resembled human adenocarcinomas and required only two genetic elements for transformation. Thus, the pre-existing differences among the starting cell types in each of these studies is likely to have contributed to the differences in their requirements for transformation as well as the transformed phenotype. As mammospheres are greatly enriched in stem/progenitor cells, and secondary mammospheres are known to harbor $>90\%$ bi-potent progenitors (Dontu and Wicha, 2005), it is likely that in our study it is these immature progenitors that underwent transformation. However, as mammospheres are heterogeneous, consisting of stem and progenitor cells of varying proliferation potential for which currently no specific markers have been identified, it is not possible to specify the precise nature of the cell that underwent transformation in our study.

Long-term *in vitro* culturing of NBLEs led to selective expansion of the tumorigenic breast CSCs. The SV40ER encodes for LT and ST antigens, which are known to inactivate tumor suppressors such as p53, pRb and PP2A (Yang *et al*., 1991; Ali and DeCaprio, 2001), and recent studies have identified a role for several oncogenes and tumor-suppressor genes in the regulation of stemness properties (Pardal *et al*., 2005). For example, down-regulation of p53 has been associated with increased self-renewal, and upregulation of stem cell markers, such as Nanog, ABCB1 and CD44 (Jerry *et al*., 2008). Other studies have shown that lower levels of p53 results in increased mammary stem/progenitors (Tao *et al*., 2011) and lack of pRb has been shown to promote expansion of multi-potent stem cells (Gutierrez *et al*., 2008). In addition, the ST antigen has been shown to activate Notch,

Hedgehog and Wnt pathways (Ali-Seyed *et al*., 2006) all of which are associated with stem cell self-renewal as well as breast carcinogenesis (Liu *et al*., 2005). Furthermore, overexpression of telomerase is also known to enhance proliferation of adult stem cells (Sarin *et al*., 2005). Thus, the introduced oncogenes are likely to have contributed to the long-term stemness properties of NBLE cells.

Recent studies have shown that induction of EMT, a critical event during metastatic tumor progression, generates mammary epithelial cells with stem cell properties (Mani *et al*., 2008). Induction of EMT increases the $CD44^+/CD24^-$ population, and increased expression of CD44 might induce EMT (Bhat-Nakshatri *et al*., 2010; Uchino *et al*., 2010). The $CD44^+/CD24^-$ fraction of NBLEs showed EMT phenotype and exhibited activated self-renewal pathways. Thus, the interplay between the introduced oncogenes and self-renewal pathways may have additionally contributed to the cancer stem-like properties of NBLE cells.

Thus, our data reveals that the introduction of two genetic elements into mammospheres suffices for their tumorigenic transformation leading to the generation of breast cancer stem-like cells. The phenotypic, molecular and functional resemblance of the mammosphere-derived tumors with naturally arising ductal adenocarcinoma strongly supports a more primitive cell as the origin for this form of breast cancer. Thus, the NBLEs provide a potent experimental tool to understand the changes associated with the transformation of immature stem/progenitor cells. These cells can be further exploited for screening drugs against breast CSCs.

Materials and methods

Mammosphere and cell culture
Mammospheres were cultured as described previously (Dey *et al*., 2009). Normal and cancerous breast tissues were obtained from Kidwai Memorial Institute of Oncology (KMIO), Bangalore, as per the Institutional Review Board and in compliance with the ethical guidelines of KMIO and Indian Institute of Science. Multiple hematoxylin and eosin staining and karyotype analysis was undertaken to confirm the normal stature of breast tissue. Mammospheres were typically passaged by trypsinization on day 7.

Sub-cloning and lentiviral transduction
The SV40ER and hTERT complementary DNA were sub-cloned into pCSCG lentiviral vector and transfected along with packaging plasmids (pHR′Δ8.2. and pCMV-VSVG) into HEK293 T cells using Fugene-6 (Roche, Mannheim, Germany). After 48 h, viral supernatant was harvested. Primary T1 mammospheres were enzymatically dissociated into single cells, re-suspended in viral supernatant containing 8 μg/ml protamine sulfate and 0.1 M HEPES buffer and seeded in 12-well ultra-low attachment plates (Corning, Lowell, MA, USA). Spin infection was performed for 60 min at 37 °C at 1200 r.p.m. followed by further incubation with virus for 5 h in 37 °C incubator. Thereafter, the cells were spun down and re-suspended in Dulbecco's modified Eagle's medium-F12 media with growth factors. After 12 h of first infection, second infection was carried out similarly, resulting in 40–50% infection efficiency, as verified by green fluorescent protein co-expressed by pCSCG vector.

RNA isolation and RT–PCR
Total RNA was isolated using Tri-reagent (Sigma Aldrich, St Louis, MO, USA). Complementary DNA was synthesized from 2 μg of total RNA using Gene-Amp RNA PCR complementary DNA synthesis kit (Applied Biosystems, Carlsbad, CA, USA). Primers were designed using Primer3 online tool, (see Supplementary Table S1 for primer sequences). HPRT and RPL35A were used as normalizing controls.

Primary cancer tissue processing and flow cytometry
Freshly procured primary cancer tissues were mechanically and enzymatically digested using 1 mg/ml Collagenase (Sigma Aldrich) and 100 U/ml Hyaluronidase (Calbiochem, Darmstadt, Germany) at 37 °C for 16–18 h with rotation. Organoids were pelleted down and resuspended in Dulbecco's modified Eagle's medium-F12 with growth factors (10 ng/ml hEGF, 1 mg/ml hydrocortisone, 10 mg/ml insulin, 4 ng/ml heparin (Sigma Aldrich) and B27 (Invitrogen, Carlsbad, CA, USA)). After 6–8 h, the organoids were trypsinized, filtered through 70 μm cell strainer (BD Biosciences, Franklin Lakes, NJ, USA) and single cells were incubated in 37 °C incubator for 60 min for surface antigen recovery, and stained with CD44-PE (BD Biosciences) and CD24-Alexa Fluor 610 (Invitrogen) for 45 min at 4 °C in dark. Stained cells were sorted in BD FACS-ARIA II (BD Biosciences) or Moflo cytometer (Beckman Coulter, Miami, FL, USA). Unstained cells, CD44-alone and CD24-alone stained cells served as controls to set gates.

Differentiation assays
Cells were seeded on regular tissue culture plates in differentiation media (Dulbecco's modified Eagle's medium-F12 media containing 10% fetal bovine serum, 100 nM all-trans retinoic acid and reduced growth factors). These cells were fixed after 4 days and immunostained. For dual staining with CK14 and CK18, cells were seeded at clonal densities (500 cells/ml) on regular tissue culture plates and allowed to grow for 8–10 days. For 3D differentiation assays, 8-well chamber slides or 96-well plates were coated with 50 μl matrigel (BD Biosciences) and allowed to dry for 30 min. Cells were re-suspended in matrigel assay media containing 100 nM trans-retinoic acid, 5% matrigel, 5% fetal bovine serum and allowed to grow for 12–14 days with media replenishment every fourth day. All immunostaining assays included negative controls as shown in Supplementary Figure S1.

Karyotype analysis
Karyotyping was undertaken at Anand Diagnostic Laboratory, Bangalore, India, and analyzed by expert cytogeneticists. Metaphase-spreads were analyzed using the karyotype analysis software from Applied Spectral Imaging, Migdal Ha'Emek, Israel (see detailed protocol under Supplementary Information).

Microarray analysis
Microarray experiments were undertaken using the human 4X44K array (AMADID, Agilent P/N G2534-60011, Agilent Technologies, Santa Clara, CA, USA) either in-house or at Genotypic Technology Pvt. Ltd, Bangalore, India. The images were scanned with Agilent Technologies Scanner G2505C, and were processed and normalized using the GeneSpring-GX 11.0.1 software (Agilent Technologies). The complete microarray data can be accessed at 'http://www.ncbi.nlm.nih.gov/geo/query/acc.cgi?acc=GSE22169' with accession number: 'GSE22169' and detailed experimental procedures are described in supplementary information.

Conflict of interest

The authors declare no conflict of interest.

Acknowledgements

We thank Dr Robert A Weinberg (Whitehead Institute) for hTERT cDNA, HMLE and HMLER cells and Dr Inder M Verma (Salk Institute) for pCSCG lentiviral vector. We acknowledge Swati Maiti for insightful discussions, and thank D Alaguraj, Drs Omana Joy, William Surin (IISc) and H Krishnamurthy (NCBS) for help with flow cytometry. We also thank Dr Paturu Kondaiah and Imran Khan (IISc), and Mohammed Aiyaz (Genotypic India Pvt. Ltd) for help with microarray experiments and data analysis. This work was largely supported by research grants from DBT to AR for equipment and consumables. We acknowledge the confocal, IRIS, FACS and animal facilities at IISc, and grants from UGC to the Department of MRDG, IISc.

References

Al-Hajj M, Wicha MS, Benito-Hernandez A, Morrison SJ, Clarke MF. (2003). Prospective identification of tumorigenic breast cancer cells. *Proc Natl Acad Sci USA* **100**: 3983–3988.

Ali SH, DeCaprio JA. (2001). Cellular transformation by SV40 large T antigen: interaction with host proteins. *Semin Cancer Biol* **11**: 15–23.

Ali-Seyed M, Laycock N, Karanam S, Xiao W, Blair ET, Moreno CS. (2006). Cross-platform expression profiling demonstrates that SV40 small tumor antigen activates Notch, Hedgehog, and Wnt signaling in human cells. *BMC Cancer* **6**: 54.

Ayyanan A, Civenni G, Ciarloni L, Morel C, Mueller N, Lefort K *et al*. (2006). Increased Wnt signaling triggers oncogenic conversion of human breast epithelial cells by a Notch-dependent mechanism. *Proc Natl Acad Sci USA* **103**: 3799–3804.

Ben-Porath I, Thomson MW, Carey VJ, Ge R, Bell GW, Regev A *et al*. (2008). An embryonic stem cell-like gene expression signature in poorly differentiated aggressive human tumors. *Nat Genet* **40**: 499–507.

Bhat-Nakshatri P, Appaiah H, Ballas C, Pick-Franke P, Goulet Jr R, Badve S *et al*. (2010). SLUG/SNAI2 and tumor necrosis factor generate breast cells with CD44+/CD24- phenotype. *BMC Cancer* **10**: 411.

Bissell MJ, Weaver VM, Lelievre SA, Wang F, Petersen OW, Schmeichel KL. (1999). Tissue structure, nuclear organization, and gene expression in normal and malignant breast. *Cancer Res* **59**: 1757–1763s; discussion 1763s-1764s.

Charafe-Jauffret E, Ginestier C, Birnbaum D. (2009). Breast cancer stem cells: tools and models to rely on. *BMC Cancer* **9**: 202.

Chu PG, Weiss LM. (2002). Keratin expression in human tissues and neoplasms. *Histopathology* **40**: 403–439.

Creighton CJ, Li X, Landis M, Dixon JM, Neumeister VM, Sjolund A *et al*. (2009). Residual breast cancers after conventional therapy display mesenchymal as well as tumor-initiating features. *Proc Natl Acad Sci USA* **106**: 13820–13825.

Dey D, Saxena M, Paranjape AN, Krishnan V, Giraddi R, Kumar MV *et al*. (2009). Phenotypic and functional characterization of human mammary stem/progenitor cells in long term culture. *PLoS One* **4**: e5329.

Dimri G, Band H, Band V. (2005). Mammary epithelial cell transformation: insights from cell culture and mouse models. *Breast Cancer Res* **7**: 171–179.

Dontu G, Abdallah WM, Foley JM, Jackson KW, Clarke MF, Kawamura MJ *et al*. (2003). *In vitro* propagation and transcriptional profiling of human mammary stem/progenitor cells. *Genes Dev* **17**: 1253–1270.

Dontu G, Wicha MS. (2005). Survival of mammary stem cells in suspension culture: implications for stem cell biology and neoplasia. *J Mammary Gland Biol Neoplasia* **10**: 75–86.

Elenbaas B, Spirio L, Koerner F, Fleming MD, Zimonjic DB, Donaher JL *et al*. (2001). Human breast cancer cells generated by oncogenic transformation of primary mammary epithelial cells. *Genes Dev* **15**: 50–65.

Gudjonsson T, Villadsen R, Nielsen HL, Ronnov-Jessen L, Bissell MJ, Petersen OW. (2002). Isolation, immortalization, and characterization of a human breast epithelial cell line with stem cell properties. *Genes Dev* **16**: 693–706.

Gutierrez GM, Kong E, Sabbagh Y, Brown NE, Lee JS, Demay MB *et al*. (2008). Impaired bone development and increased mesenchymal progenitor cells in calvaria of RB1-/- mice. *Proc Natl Acad Sci USA* **105**: 18402–18407.

Ince TA, Richardson AL, Bell GW, Saitoh M, Godar S, Karnoub AE *et al*. (2007). Transformation of different human breast epithelial cell types leads to distinct tumor phenotypes. *Cancer Cell* **12**: 160–170.

Jerry DJ, Tao L, Yan H. (2008). Regulation of cancer stem cells by p53. *Breast Cancer Res* **10**: 304.

Liao MJ, Zhang CC, Zhou B, Zimonjic DB, Mani SA, Kaba M *et al*. (2007). Enrichment of a population of mammary gland cells that form mammospheres and have *in vivo* repopulating activity. *Cancer Res* **67**: 8131–8138.

Liu S, Dontu G, Wicha MS. (2005). Mammary stem cells, self-renewal pathways, and carcinogenesis. *Breast Cancer Res* **7**: 86–95.

Mani SA, Guo W, Liao MJ, Eaton EN, Ayyanan A, Zhou AY *et al*. (2008). The epithelial-mesenchymal transition generates cells with properties of stem cells. *Cell* **133**: 704–715.

Morel AP, Lievre M, Thomas C, Hinkal G, Ansieau S, Puisieux A. (2008). Generation of breast cancer stem cells through epithelial-mesenchymal transition. *PLoS One* **3**: e2888.

Muschler J, Lochter A, Roskelley CD, Yurchenco P, Bissell MJ. (1999). Division of labor among the alpha6beta4 integrin, beta1 integrins, and an E3 laminin receptor to signal morphogenesis and beta-casein expression in mammary epithelial cells. *Mol Biol Cell* **10**: 2817–2828.

O'Brien CA, Kreso A, Jamieson CH. (2010). Cancer stem cells and self-renewal. *Clin Cancer Res* **16**: 3113–3120.

Pardal R, Clarke MF, Morrison SJ. (2003). Applying the principles of stem-cell biology to cancer. *Nat Rev Cancer* **3**: 895–902.

Pardal R, Molofsky AV, He S, Morrison SJ. (2005). Stem cell self-renewal and cancer cell proliferation are regulated by common networks that balance the activation of proto-oncogenes and tumor suppressors. *Cold Spring Harb Symp Quant Biol* **70**: 177–185.

Phesse TJ, Clarke AR. (2009). Normal stem cells in cancer prone epithelial tissues. *Br J Cancer* **100**: 221–227.

Ponti D, Zaffaroni N, Capelli C, Daidone MG. (2006). Breast cancer stem cells: an overview. *Eur J Cancer* **42**: 1219–1224.

Rochlitz CF, Scott GK, Dodson JM, Liu E, Dollbaum C, Smith HS *et al*. (1989). Incidence of activating ras oncogene mutations associated with primary and metastatic human breast cancer. *Cancer Res* **49**: 357–360.

Rodriguez Salas N, Gonzalez Gonzalez E, Gamallo Amat C. (2010). Breast cancer stem cell hypothesis: clinical relevance (answering breast cancer clinical features). *Clin Transl Oncol* **12**: 395–400.

Sarin KY, Cheung P, Gilison D, Lee E, Tennen RI, Wang E *et al*. (2005). Conditional telomerase induction causes proliferation of hair follicle stem cells. *Nature* **436**: 1048–1052.

Shackleton M. (2010). Normal stem cells and cancer stem cells: similar and different. *Semin Cancer Biol* **20**: 85–92.

Tan BT, Park CY, Ailles LE, Weissman IL. (2006). The cancer stem cell hypothesis: a work in progress. *Lab Invest* **86**: 1203–1207.

Tao L, Roberts AL, Dunphy KA, Bigelow C, Yan H, Jerry DJ. (2011). Repression of mammary stem/progenitor cells by P53 is

mediated by Notch and separable from apoptotic activity. *Stem Cells* **29**: 119–127.

Uchino M, Kojima H, Wada K, Imada M, Onoda F, Satofuka H *et al*. (2010). Nuclear beta-catenin and CD44 upregulation characterize invasive cell populations in non-aggressive MCF-7 breast cancer cells. *BMC Cancer* **10**: 414.

Wazer DE, Liu XL, Chu Q, Gao Q, Band V. (1995). Immortalization of distinct human mammary epithelial cell types by human papilloma virus 16 E6 or E7. *Proc Natl Acad Sci USA* **92**: 3687–3691.

Woods C, LeFeuvre C, Stewart N, Bacchetti S. (1994). Induction of genomic instability in SV40 transformed human cells: sufficiency of the N-terminal 147 amino acids of large T antigen and role of pRB and p53. *Oncogene* **9**: 2943–2950.

Woodward WA, Chen MS, Behbod F, Rosen JM. (2005). On mammary stem cells. *J Cell Sci* **118**: 3585–3594.

Yang SI, Lickteig RL, Estes R, Rundell K, Walter G, Mumby MC. (1991). Control of protein phosphatase 2A by simian virus 40 small-t antigen. *Mol Cell Biol* **11**: 1988–1995.

Zhao X, Malhotra GK, Lele SM, Lele MS, West WW, Eudy JD *et al*. (2010). Telomerase-immortalized human mammary stem/progenitor cells with ability to self-renew and differentiate. *Proc Natl Acad Sci USA* **107**: 14146–14151.

Supplementary Information accompanies the paper on the Oncogene website (http://www.nature.com/onc)